Structural and Biochemical Characterization of Flavoredoxin from the Archaeon *Methanosarcina acetivorans*[†,‡]

Suharti Suharti,[§,||,⊥] Katsuhiko S. Murakami,[*,§,⊥] Simon de Vries,[#] and James G. Ferry[*,§]

Department of Biochemistry and Molecular Biology, The Pennsylvania State University, University Park, Pennsylvania 16802, Department of Biotechnology, Delft University of Technology, Julianalaan 67, 2628 BC Delft, The Netherlands, and Department of Chemistry, State University of Malang, Malang 65145, East Java-Indonesia

Received May 29, 2008; Revised Manuscript Received September 13, 2008

ABSTRACT: Flavoredoxin is a FMN-containing electron transfer protein that functions in the energy-yielding metabolism of *Desulfovibrio gigas* of the Bacteria domain. Although characterization of this flavoredoxin is the only one reported, a database search revealed homologues widely distributed in both the Bacteria and Archaea domains that define a novel family. To improve our understanding of this family, a flavoredoxin from *Methanosarcina acetivorans* of the Archaea domain was produced in *Escherichia coli* and biochemically characterized, and a high-resolution crystal structure was determined. The protein was shown to be a homodimer with a subunit molecular mass of 21 kDa containing one noncovalently bound FMN per monomer. Redox titration showed an E_m of −271 mV with two electrons, consistent with no semiquinone observed in the potential range studied, a result suggesting the flavoredoxin functions as a two-electron carrier. However, neither of the obligate two-electron carriers, NAD(P)H and coenzyme $F_{420}H_2$, was a competent electron donor, whereas 2[4Fe-4S] ferredoxin reduced the flavoredoxin. The X-ray crystal structure determined at 2.05 Å resolution revealed a homodimer containing one FMN per monomer, consistent with the biochemical characterization. The isoalloxazine ring of FMN was shown buried within a narrow groove ∼10 Å from the positively charged protein surface that possibly facilitates interaction with the negatively charged ferredoxin. The structure provides a basis for predicting the mechanism by which electrons are transferred between ferredoxin and FMN. The FMN is bound with hydrogen bonds to the isoalloxazine ring and electrostatic interactions with the phosphate moiety that, together with sequence analyses of homologues, indicate a novel FMN binding motif for the flavoredoxin family.

Flavoredoxin (Flr)[1] is a FMN-containing flavoprotein that was first isolated from the sulfate-reducing species *Desulfovibrio gigas* of the Bacteria domain (*1*). Although coordinates of the crystal structure of *Desulfovibrio vulgaris* Flr are deposited in the Protein Data Bank (PDB) (entry 2D5M), *D. gigas* Flr remains the only biochemically characterized Flr. Unlike most other FMN-containing proteins, the sequence of Flr from *D. gigas* has no recognizable flavin binding motif and does not form a stable semiquinone (*1, 2*). A BLAST search of the databases reported in 2000 indicated that the *D. gigas* Flr is the most similar in sequence (19−27%) to members of the family of NADH-dependent flavin reductases, although the Flr was unable to oxidize either NADH or NADPH (*2*). Thus, it appears that flavoredoxins comprise a novel class of flavoproteins. The *D. gigas* Flr couples electron transfer from ferredoxin or flavodoxin to the dissimilatory sulfite reductase called desulfoviridin, yielding the maximum efficiency for the reconstituted electron transfer chain between hydrogenase and desulfoviridin (*1*). A mutant of *D. gigas* with the *flr* gene deleted exhibited a reduced level of growth with sulfite as the electron acceptor and lactate as the electron donor, and the level of consumption of H_2 by the mutant was reduced ∼50% with thiosulfate as the electron acceptor (*3*). Thus, Flr is implicated as an important electron carrier in the energy-yielding pathway of sulfate reduction for *D. gigas* of the Bacteria domain, and this is the only physiological function reported for any Flr.

Genomic sequencing has revealed annotations for flavoredoxins in anaerobic microbes from the Bacteria and Archaea domains (*4*), including diverse methane-producing species of the Archaea domain (*Methanosarcina acetivorans*, *Methanosarcina mazei*, *Methanosarcina barkeri*, *Methanospirillum hungatei*, *Methanosphaera stadmanae*, *Methanoregula boo-*

[†] The research was supported by National Science Foundation Grant MCB-0110762 to J.G.F. and National Institutes of Health Grant GM071897 to K.S.M.

[‡] The atomic coordinates and structure factors have been deposited in the Protein Data Bank as entry 3BNK.

* To whom correspondence should be addressed. J.G.F.: Department of Biochemistry and Molecular Biology, Eberly College of Science, The Pennsylvania State University, 205 South Frear Laboratory, University Park, PA 16802-4500; phone, (814) 863-5721; fax, (814) 863-6217; e-mail, jgf3@psu.edu. K.S.M.: Department of Biochemistry and Molecular Biology, The Pennsylvania State University, 006 Althouse Laboratory, University Park, PA 16802-4500; phone, (814) 865-2758; fax, (814) 865-2759; e-mail, kum14@psu.edu.

[§] The Pennsylvania State University.

[||] State University of Malang.

[⊥] These authors contributed equally to this work.

[#] Delft University of Technology.

[1] Abbreviations: Flr, flavoredoxin; Cdh, CO dehydrogenase/acetyl-CoA synthase.

10.1021/bi801012p CCC: $40.75
Published on Web 10/09/2008

nei, and *Methanoculleus marisnigri*). The enzymology and molecular biology of carbon transfer reactions leading to methane are well-resolved (*5, 6*); however, less is known about electron transport, especially for the pathway of conversion of acetate to methane which is responsible for at least two-thirds of the nearly 1 billion metric tons of methane produced annually in Earth's biosphere (*7*). Only two acetate-utilizing genera are known, *Methanosarcina* and *Methanothrix*, of which the pathway for methanogenesis is best understood for the former (*6*). The genomes of *Methanosarcina* species are annotated with the electron carrier proteins ferredoxin, flavodoxin, rubredoxin, iron−sulfur flavoprotein, and Flr (*4*); however, only the roles of ferredoxin and iron−sulfur flavoprotein have been reported for any acetate-utilizing species. The genome of *M. acetivorans* harbors three genes (MA0328, MA2295, and MA3965) annotated as encoding flavoredoxins (*4*) that we have designated Ma-Flr-1, Ma-Flr-2, and Ma-Flr-3, respectively. Here we report on the biochemical properties and crystal structure of Ma-Flr-1 that to the best of our knowledge is the first Flr characterized from any methane-producing species and the Archaea domain.

MATERIALS AND METHODS

Cloning and Overexpression. The open reading frame (ORF) of the *Ma-Flr-1* encoding gene was amplified by PCR from *M. acetivorans* genomic DNA. A pair of sense (5′TTGTTGCATATGGCAGAGAAAATCAAG) and antisense (5′GATGATCTCGAGTCTTTTCTCCATCAGGCTTTTAA) primers was used to amplify the *Ma-Flr-1* gene and to introduce the *Nde*I and *Xho*I restriction sites (underlined sequences). The PCR fragment was cloned into the pET22b(+) (Novagen) vector. The C-terminal six-histidine-tagged recombinant protein was expressed with *Escherichia coli* Rosetta pLacI cells. The transformed cells were cultured at 37 °C in Luria-Bertani broth containing 100 mg of ampicillin per liter. When the OD_{600} reached 0.7, Ma-Flr-1 was expressed by the addition of 0.5 mM IPTG. The culture was incubated for 16 h at 16 °C. Cells were harvested by centrifugation and stored at −80 °C.

Purification of Recombinant Ma-Flr-1. The purification of Ma-Flr-1 was conducted aerobically at 21 °C. Approximately 15 g of thawed cells was resuspended in 20 mM potassium phosphate buffer (pH 7.4) containing 500 mM NaCl and 20 mM imidazole. DNase and 0.25 mM phenylmethanesulfonyl fluoride were then added and the cells lysed by being passed twice through a French pressure cell at 110 MPa. Cell debris and membranes were removed by centrifugation at 100000*g* for 45 min at 4 °C. The supernatant was filtered and loaded onto a Ni Sepharose high-performance column (GE Healthcare) equilibrated with phosphate buffer containing 500 mM NaCl and 20 mM imidazole. The column was then washed with 3 column volumes of phosphate buffer containing 500 mM NaCl, 50 mM imidazole, and 25% glycerol. After the column was washed with another column volume of the same buffer without glycerol, Ma-Flr-1 was eluted with phosphate buffer containing 500 mM NaCl and 150 mM imidazole. The eluted yellow fraction was dialyzed at 4 °C against 50 mM Tris-HCl (pH 8) containing 300 mM NaCl using a 3.5 kDa cutoff cellulose membrane. Ma-Flr-1 was then concentrated using a Centricon YM-10000 instrument, and the concentrated Ma-Flr-1 was stored at −80 °C.

Biochemical Analysis of Ma-Flr-1. For the analysis of noncovalently bound flavin, purified Ma-Flr-1 was denatured by either adding trichloroacetic acid to a final concentration of 5% or boiling for 5 min. The precipitated protein was removed by centrifugation, and the supernatant was filtered using an Ultrafree-MC 5000 NMWL filter unit (Millipore). The filtrate was then neutralized by adding 2 M K_2HPO_4. The free flavin concentration was determined spectroscopically using an extinction coefficient of 12.2 mM^{-1} cm^{-1} at 452 nm (oxidized form) (*8*). The flavin type was determined by TLC using a silica gel matrix (Fluka) with an *n*-butanol/acetic acid/water mixture (4:1:5) as the mobile phase. The protein concentration was quantified by the bicinchoninic assay (Pierce). Anaerobic dye-mediated redox titrations were carried out in a stoppered quartz cuvette exactly as described previously (*1*) using the same mediators except the titration was conducted at 22 °C in 50 mM Tris-HCl (pH 7.5). Briefly, to a solution of 25 μM flavoredoxin in 50 mM Tris-HCl (pH 7.5) were added the following redox mediators each at a concentration of 1 μM: methylene blue, indigo tetrasulfonate, indigo disulfonate, 2-hydroxy-1,4-naphthoquinone, anthraquinone 2-sulfonate, neutral red, benzyl viologen, and methyl viologen. The solution was kept anaerobic by being continuously flushed with Argon 6.0. Reductive titrations were performed by adding small aliquots from a freshly prepared anaerobic sodium dithionite solution and oxidative titrations by adding anaerobic potassium ferricyanide. UV−vis spectra were recorded with a HP8253 photodiode array spectrometer. Both a platinum electrode and an Ag/AgCl electrode were used to measure the redox potential. The electrodes were calibrated with a saturated solution of quinhydrone at pH 4.0 and 7.0. The quoted redox potentials are versus the normal hydrogen electrode (NHE).

The ferredoxin-dependent reduction of Ma-Flr-1 was assessed by regenerating reduced ferredoxin with CO dehydrogenase/acetyl-CoA synthase (Cdh) purified from *M. acetivorans* (a gift of M. Wang). A 500 μL reaction mixture containing 50 mM Tris-HCl (pH 8), 100 μM Ma-Flr-1, and the indicated concentrations of 2[4Fe-4S] ferredoxin from *Clostridium pasteurianum* (Sigma) was placed in a 1.5 mL anaerobic cuvette sealed with a rubber stopper. The reaction mixture was then equilibrated with 1 atm of CO or N_2 for the control reaction. Approximately 250 ng of Cdh from *M. acetivorans* was then added to the reaction mixture. The activity was followed by monitoring the decrease in absorbance of Ma-Flr-1 at 452 nm ($\varepsilon_{452} = 8.5$ mM^{-1} cm^{-1}). The same procedure was followed to assay CO- or H_2-dependent reduction of Ma-Flr-1 catalyzed by crude cell-free extract except ferredoxin and Cdh were replaced with 50 μL of extract (12 mg of protein/mL) prepared as described previously (*9*).

The NADH, NADPH, and $F_{420}H_2$ reduction of Ma-Flr-1 was assessed in an anaerobic chamber (Coy Manufacturing) containing 95% N_2 and 5% H_2. The 500 μL reaction mixture containing 50 mM Tris-HCl (pH 8) and 100 μM Ma-Flr-1 was placed in a 1.5 mL cuvette, and the electron donors (200 μM final concentration) were added to initiate the reaction that was followed by recording the absorbance of NADH or NADPH at 340 nm or Ma-Flr-1 at 452 nm. Coenzyme F_{420}

Table 1: Stimulation by Ferredoxin of the Reduction of Ma-Flr-1 with CO Dehydrogenase/Acetyl-CoA Synthase

[ferredoxin] (μM)	rate (μmol/min)[a]	[ferredoxin] (μM)	rate (μmol/min)[a]
0	1.5	4.8	29
0.8	14	6.3	32
2.3	21	12	82

[a] The rate was determined by monitoring the decrease in absorbance of 100 μM Ma-Flr-1 at 452 nm. See Materials and Methods.

was chemically reduced with sodium borohydride as described previously (*10*).

The ability of Ma-Flr-1 to reduce FMN, FAD, or riboflavin was assessed by reducing Ma-Flr-1 with the reduced ferredoxin regenerating system described above. The reaction mixture containing 50 mM Tris-HCl (pH 8), 1 μM Ma-Flr-1, 100 μg of ferredoxin from *C. pasteurianum*, and the electron acceptor at 100 μM was placed in a 1.5 mL anaerobic cuvette sealed with a rubber stopper. The reaction mixture was then equilibrated with 1 atm of CO followed by the addition of 2 μg of Cdh from *Methanosarcina thermophila* (a gift of D. Grahame) to initiate the reaction. Reduction of the electron acceptors was monitored at 452 nm. The ferric iron reductase activity of Ma-Flr-1 was determined as follows. Ma-Flr-1 (100 μM) was reduced by the reduced ferredoxin regenerating system described above. After complete reduction of Ma-Flr-1, the CO atmosphere was replaced and equilibrated for 15 min with N_2. The reaction was initiated by the addition of 1 mM anaerobic ferric chloride or ferric EDTA. The reaction was monitored by following the reoxidation of Ma-Flr-1 at 452 nm.

Crystallization and Determination of the Structure of Ma-Flr-1-. Ma-Flr-1 was crystallized by vapor diffusion in hanging drops with microseeding at 22 °C against a reservoir containing 0.1 M Tris-HCl (pH 8.0), 0.1 M NaBr, and ~30% (w/v) polyethylene glycol (PEG) 4000. Crystals reached their full size within 1 day and were yellow in color because of the presence of FMN. For cryocrystallography, the crystals were harvested from a drop and then flash-frozen by immersion in liquid nitrogen. Complete 2.05 Å resolution diffraction data (Table 1) were collected using a Rigaku RU200 instrument equipped with an R-axis IV imaging plate and processed with HKL2000 (*11*). Primitive orthorhombic space group $P2_12_12_1$ crystals (a = 62.1 Å, b = 74.8 Å, and c = 75.8 Å) contained two 21.0 kDa Flr molecules per asymmetric unit. The structure was determined by a molecular replacement {resolution range from 2.5 to 24 Å [Phaser (*12*)]}. The search model was derived from the Flr from *D. vulgaris* (PDB entry 2D5M) via removal of flexible N- and C-terminal loops (residues 1−11 and 175−186) and FMN. A molecular replacement solution includes two Flr molecules in an asymmetric unit (*Z*-scores of the top and second solutions are 9.50 and 5.67, respectively). The electron density map was calculated using phases from the molecular replacement, and it was further improved using the density modification program Resolve (*13*) which includes noncrystallographic symmetry restraints. The resulting electron density map has several deviations from the molecular replacement solution, indicating that model bias was effectively removed by density modification. The rigid body and positional refinements were performed with refmac5 (*14*), and further adjustments to the model were carried out manually. The amino acid sequence of the model was replaced with that of *M. acetivorans* Flr. Positional refinement without NCS restraint was carried out, and map improvement was facilitated by model building using O (*15*). Finally, FMN and water molecules were added to the model. The final model contains residues 2−187 of molecule A, residues 2−188 of molecule B, two FMN molecules, and 116 water molecules (R_{work} = 20.84%; R_{free} = 26.50%). PROCHECK (*16*) revealed that all residues are in allowed regions.

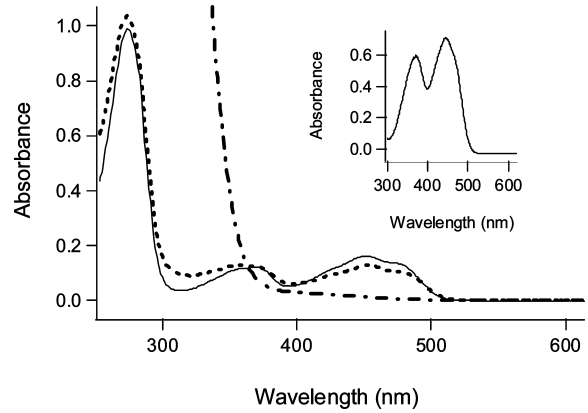

FIGURE 1: UV−vis spectra of Ma-Flr-1: oxidized (—), partially reduced with sodium dithionite (---), and fully reduced with sodium dithionite (−•−). The inset shows the spectrum of the extracted FMN.

Homology analysis, sequence alignment, phylogenetic tree construction, and BLAST analyses were conducted using the SIB Blast Network Service with MA0328 (accession number Q8TTU7) as the query against all available sequences at the UniProt Knowledgebase (Swiss-Prot + TrEMBL) acquired on January 15, 2008 (*17*). The BLAST results with *E* values of $\leq 5 \times 10^{-10}$ (sequence identity of ≥26%) were then selected for multiple-sequence alignment and phylogenetic tree construction. Multiple alignments were done with clustalX version 1.83, and the phylogenetic tree was constructed with MEGA version 3.1 using the minimum evolution methods.

RESULTS

Biochemical Characterization. M. acetivorans Ma-Flr-1 was produced in *E. coli* and purified to homogeneity as determined by SDS−PAGE. The protein had a subunit molecular mass of approximately 21 kDa determined by SDS−PAGE and a native molecular mass of 45 ± 0.5 kDa determined by molecular sieve chromatography, results indicating that Ma-Flr-1 is a homodimer. The as-purified protein appeared yellow and had an UV−visible spectrum that exhibited absorbance maxima at 375 and 452 nm with shoulders at 425 and 475 nm typical of flavoproteins (Figure 1). The monomeric extinction coefficient determined at 452 nm was 8.5 mM^{-1} cm^{-1}. The UV−visible spectrum (Figure 1, inset) of the chromophore released by boiling Ma-Flr-1 for 5 min or by addition of 20% TCA indicated that Ma-Flr-1 contains a noncovalently bound flavin. The released flavin migrated to the same position as FMN on thin-layer chromatograms, and treatment with pyrophosphatase did not increase the fluorescence emission at 550 nm, results which indicated that the type of flavin in Ma-Flr-1 is FMN. The

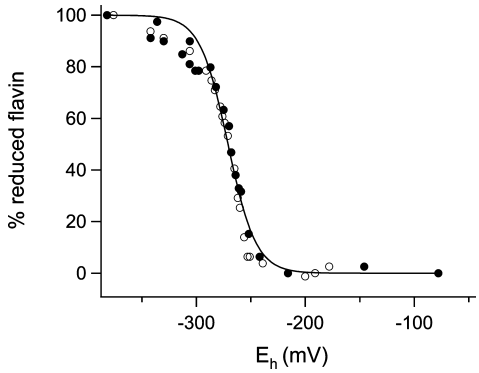

FIGURE 2: Redox titration of Ma-Flr-1: reduction (○) and reoxidation (●). The line is a fitted line to the Nernst equation with $n = 2$.

native dimer contained two FMNs. Spectra of Ma-Flr-1 partially reduced with dithionite did not exhibit increased absorbance in the vicinity of 375 and 600 nm that would have indicated a neutral (red) semiquinone, or a shift of the 375 nm peak to lower wavelengths that would have indicated an anionic (blue) semiquinone (Figure 1). Further, redox titration indicated a value of two electrons, and no absorbance was observed indicative of a red or blue flavosemiquinone in the redox potential range that was studied (Figure 2). The scatter in the data points at redox potentials below −300 mV was the result of dye interference, mainly to benzyl viologen. The results suggest that the fully reduced hydroquinone is more thermodynamically stable than the semiquinone state which is short-lived and undetectable. The fitted curve of the redox titration indicated an E_m value of −271 ± 0.9 mV.

The physiological electron donors NADH, NADPH, and $F_{420}H_2$ were incompetent in reducing Ma-Flr-1. However, crude cell-free extract of *M. acetivorans* catalyzed CO-dependent reduction at a rate of 5.2 nmol min^{-1} (mg of cell-free extract protein)$^{-1}$, indicating that Ma-Flr-1 functions as an electron carrier. H_2 was unable to replace CO as the electron donor for reduction of Ma-Flr-1 by extracts of acetate-, methanol-, or trimethylamine-grown cells (data not shown), consistent with the low levels of H_2-dependent activity and no apparent role for H_2 or hydrogenase during growth of *M. acetivorans* with acetate (*9, 18*). These results suggest that electron transport to Ma-Flr-1 is linked to Cdh that is central to the pathway for conversion of acetate to methane in *Methanosarcina* species (*18, 19*). Cdh purified from *M. acetivorans* slowly catalyzed the CO-dependent reduction of Ma-Flr-1 that was stimulated severalfold with increasing concentrations of 2[4Fe-4S] ferredoxin from *C. pasteurianum* (Table 1). The results indicate that 2[4Fe-4S] ferredoxin is an electron acceptor for *M. acetivorans* Cdh, consistent with the Cdh from other *Methanosarcina* species (*20, 21*), and that ferredoxin is an electron donor to Ma-Flr-1, consistent with that reported for *D. gigas* Flr (*1*). FMN, FAD, riboflavin, ferric iron, and chelated ferric iron were incompetent in accepting electrons from reduced Ma-Flr-1.

Overall Structure. The X-ray crystal structure of Ma-Flr-1 was determined at 2.05 Å resolution by using molecular replacement with a search model derived from *D. vulgaris* Flr (PDB entry 2D5M). The crystal structure of Ma-Flr-1 forms a homodimer (Figure 3A), consistent with results obtained from size-exclusion column chromatography. Each monomer has an almost identical structure with a rmsd of 0.4 Å (186 residues). The Ma-Flr-1 monomer consists of an α/β-core structure with N- and C-terminal tails. The core consists of a six-stranded antiparallel β-barrel and capping α-helices. The N- and C-terminal tails form clamps that join the monomers to form a dimer. Each monomer holds one FMN molecule, which is also consistent with the biochemical results reported here. The surface of Ma-Flr-1 is negatively charged, except the area near the FMN binding pocket which is positively charged (Figure 3B).

FMN Binding Site. Flavoredoxins have no recognizable FMN binding motif, although roles for residues were suggested on the basis of a homology model of *D. gigas* Flr (*22*). The crystal structure of Ma-Flr-1 from *M. acetivorans* unambiguously reveals a FMN binding pocket formed as a groove located near the dimer interface (Figure 3A). The FMN is surrounded by two α-helices (α1 and α2) and five β-strands (β1, β2, β3, β4, and β8) from one monomer in addition to a C-terminal tail from the other monomer. The isoalloxazine ring of FMN is buried within a narrow groove ~10 Å below the protein surface, and this is the only possible route from the protein surface to the FMN reaction center. The *si* face of the isoalloxazine ring is buried, while the *re* face is exposed to solvent (Figures 3C and 4). The ribityl phosphate moiety of FMN lies along the β2 strand, whereas the phosphate group is clamped between helices α1 and α2 (Figure 3A). FMN binding is achieved by only noncovalent bonds, including 11 hydrogen bonds and five van der Waals interactions (Figure 3C). The 2,4-pyrimidinedione edge of the isoalloxazine ring forms hydrogen bonds with the side chain of His55 (at N1) and the main chain of Gly35 (at O4 and N5), Trp36 (at O4), Gly50 (at N3), and Asn52 (at O2). The dimethylbenzene edge of the isoalloxazine ring is surrounded by van der Waals interactions, including side chains of Leu162 and Leu180. O4* and O5* of the ribityl moiety interact via hydrogen bonds with the main chain of Val86 and the side chain of Lys93, respectively. The phosphate moiety forms four salt bridges with the side chains of Asn30, Thr57, Ser87, and Lys93 and two hydrogen bonds with the main chains of Tyr56 and Gly88. A sequence alignment (Figure S1 of the Supporting Information) shows that Ma-Flr-1 residues interacting with the phosphate are conserved in *D. gigas* Flr (Asn29, Thr56, Ser86, Gly87, and Lys92), a result consistent with important roles for these conserved residues in binding the FMN of diverse flavoredoxins. Indeed, *D. gigas* Flr residues Asn29, Thr56, and Lys92 were shown to be important for binding the phosphate of FMN (*22*).

Phylogeny and FMN Binding Site Consensus. A previous PROSITE database search reported in 2000 revealed no known flavin binding motif in the bacterial *D. gigas* Flr; however, because of its homology with the products of genes annotated as flavin reductases, the *D. gigas* Flr was postulated to be a member of the flavin reductase family with an unknown novel flavin binding motif (*2*). A BLAST search of the most recent databases identified 102 proteins homologous to the bacterial *D. gigas* Flr with a level of identity equal to or greater than 26% (*E* value of $\leq 5 \times 10^{-10}$) (Figure S2 of the Supporting Information). All of the homologues have a conserved motif (N-X_{54-57}-G-X_2-S-G-X_{4-10}-K) containing residues in Ma-Flr-1 (Asn30, Ser87, Gly88, and Lys93) and the archetype Flr from *D. gigas* (Asn29 and Lys92) implicated in binding FMN. An alignment of representative sequences showing the motif is

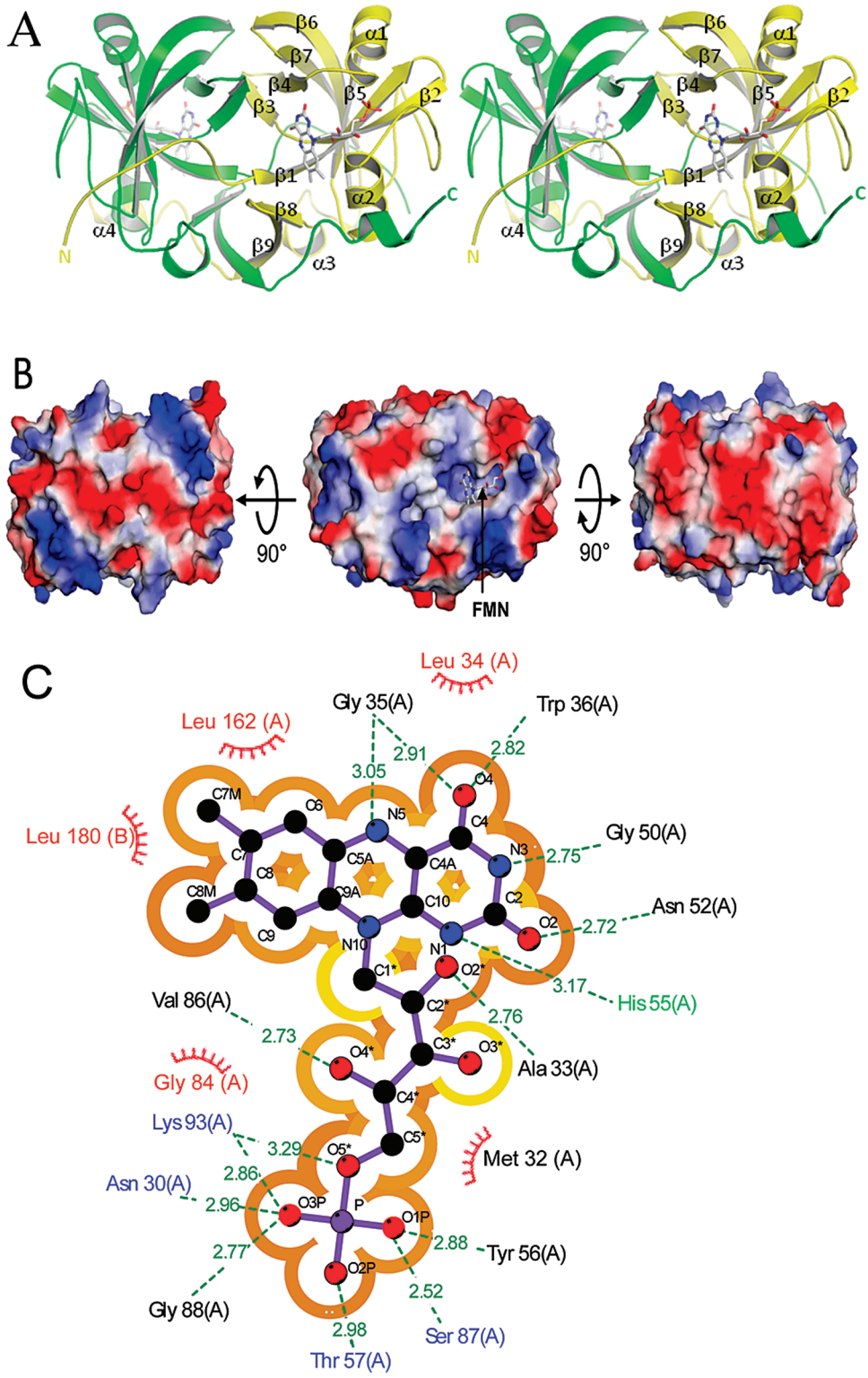

FIGURE 3: Structure of Ma-Flr-1. (A) Stereo ribbon diagram of Ma-Flr-1 representing the dimeric structure with the individual monomers colored green or yellow. The FMN molecule is drawn in stick diagram with oxygen atoms colored red, nitrogen atoms blue, carbon atoms gray, and the phosphorus atom orange. (B) Interaction between FMN and amino acid residues. Amino acid residues forming side chain hydrogen bonds are colored green; residues forming main chain hydrogen bonds are colored black, and amino acid residues forming salt bridges are colored green. Amino acid residues forming hydrophobic interactions are colored red. Residues His55 and Ala33 both form hydrophobic interactions in addition to hydrogen bonds. The solvent accessibility of FMN was calculated with NACCESS. Buried areas are colored orange and accessible areas yellow. (C) Electrostatic potential maps of the surface of Ma-Flr-1. Blue indicates positive charge and red negative charge.

shown in Figure S1 of the Supporting Information. Sequence alignments also showed that Gly84 of Ma-Flr-1 is strictly conserved among all the homologues. Although Gly84 is not involved in FMN binding, lacking a C_β atom at this position may be important for producing the space necessary to accommodate FMN. Thus, the conserved motif identifies a candidate for the previously proposed (*2*) unknown novel FMN binding motif.

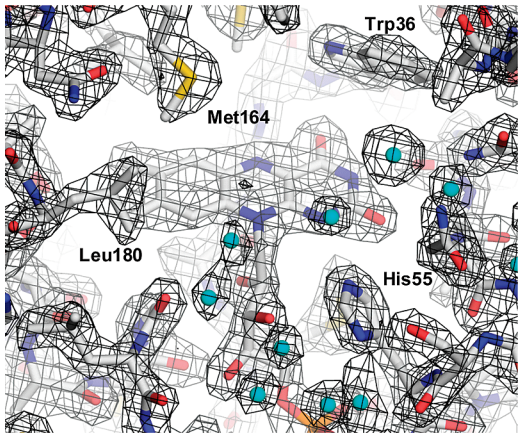

FIGURE 4: $2F_o - F_c$ electron density map of Ma-Flr-1 at 2.05 Å resolution. The map (black mesh, 1.5σ) is superimposed on the final structure. The protein and FMN are shown as a stick model, and waters are shown as cyan spheres. The orientation depicted in this figure is similar to that of Figure 3 showing the FMN binding pocket of monomer A from the protein surface. Several amino acid residues interacting with FMN are labeled, including Lys180 from monomer B.

The homologues shown in Figure S2 of the Supporting Information are annotated as Flr, flavin reductase, NADPH: flavin oxidoreductase, flavin reductase-like protein FMN binding domain, or uncharacterized proteins. Only the Flr from *D. gigas* has been characterized. None of the homologues contain a known flavin binding motif, although all contain the proposed novel FMN-binding motif N-X_{54-57}-G-X_2-S-G-X_{4-10}-K. These results suggest that the Flr homologues shown in Figure S2 of the Supporting Information are independent of the previously proposed flavin reductases (*2*) and form a novel family.

The phylogenetic tree of the archetype Flr from *D. gigas* and homologous proteins revealed two main groups (Figure S2 of the Supporting Information). Group I is found only in obligate anaerobes, while group II comprises proteins from obligate anaerobes, facultative anaerobes, and obligate aerobes. Group I is further divided into subgroups IA and IB. Ma-Flr-1 from *M. acetivorans* encoded by MA0328 (Q8TTU7) and the putative Ma-Flr-2 encoded by MA3965 (Q8TJ24) belong to group IB, while the putative Ma-Flr-3 encoded by MA2295 (Q8TNJ0) is classified in group IA together with the archetype *D. gigas* Flr from the Bacteria domain. The phylogenetic tree shows that several homologues of the flavoredoxins from *M. acetivorans* are present in *M. mazei* (Q8PTO7 and Q8PYB7) and *M. barkeri* (Q466G5 and Q45EN5), which is consistent with a physiological role for flavoredoxins in this genus.

DISCUSSION

We have investigated the oligomerization state, the redox potential of FMN, and the electron donor for Ma-Flr-1 from *M. acetivorans*, the first reported biochemical characterization of any Flr from the Archaea domain. In addition, we have determined the high-resolution crystal structure for Ma-Flr-1 which provides structural insights into FMN binding to Ma-Flr-1 and the Flr family.

Properties of Ma-Flr-1. The results reported here show that Ma-Flr-1 is a FMN-containing electron carrier protein that performs two-electron chemistry at physiological pH. The biochemical properties are similar to those of the archetype *D. gigas* Flr from the Bacteria domain (*1*), the only other characterized Flr, consistent with distinctions between Flr and the one-electron transfer protein flavodoxin. The results also demonstrate that 2[4Fe-4S] clostridial ferredoxin ($E_m = -393$ mV) is an electron donor to Ma-Flr-1, consistent with the measured redox potential of FMN in Ma-Flr-1 ($E_m = -271$ mV). Indeed, 2[4Fe-4S] ferredoxin is a prominent electron carrier in *Methanosarcina* species (*21, 23, 24*), and the genomic sequence of *M. acetivorans* (*4*) is annotated with nine ferredoxin genes encoding 2[4Fe-4S] binding motifs. The ability of Ma-Flr-1 to accept electrons from ferredoxin and perform two-electron chemistry suggests it functions as a one-electron−two-electron switch, although the physiological two-electron acceptor has not been identified.

Structural Basis of Electron Transfer between Ma-Flr-1 and Ferredoxin. A structural homology search of the DALI database identified six structures that are similar to Ma-Flr-1 (*Z*-score of >15), including *D. vulgaris* Flr (PDB entry 2D5M) which is the most similar to Ma-Flr-1. Among the six structural homologues, the only biochemical characterizations reported are those for ferric reductase from *Archaeoglobus fulgidus* (PDB entry 1I0R) (*25, 26*) and the FAD-containing flavin reductase from *Bacillus thermoglucosidasius* (PDB entry 1RZ0) (*27, 28*), both of which utilize NAD(P)H as an electron donor. In both homologues, ample spaces above the isoalloxazine ring system allow for binding NAD(P)H directly adjacent to the flavin. However, in Ma-Flr-1, there is no space above the isoalloxazine ring system of FMN, a feature that disfavors direct contact between FMN and a small molecule electron donor (Figure S3 of the Supporting Information). Thus, the structural analysis of the FMN binding pocket of Ma-Flr-1 is in agreement with the biochemical observations that NADH, NADPH, and $F_{420}H_2$ are not electron donors to Ma-Flr-1.

The structure of Ma-Flr-1 provides a basis for predicting how it interacts with ferredoxin and how electrons are transferred between ferredoxin and the FMN cofactor. The ferredoxin used in this study is an acidic protein with a pI of 3.7 (*29*), consistent with an electrostatic interaction with Ma-Flr-1 adjacent to the positively charged FMN-binding pocket. Indeed, five of the nine putative gene products in *M. acetivorans* annotated as ferredoxins have predicted pI values ranging from 3.1 to 4.1 (*4*). This postulated electrostatic interaction is consistent with that observed between ferredoxin and ferredoxin:$NADP^+$ reductase (*30, 31*). Mutations to the positively charged amino acid residues near the active center of the reductase resulted in both weakened ferredoxin binding and suboptimal electron transfer between ferredoxin and the reductase (*31*). Yet to be determined is the mechanism for two one-electron transfers from ferredoxin to the flavin. Assuming one ferredoxin binding site, the possibilities include a Cdh−ferredoxin−Ma-Flr-1 complex in which electrons are transferred sequentially or two independent short-lived collisions between reduced ferredoxin and Ma-Flr-1.

Since the FMN in Ma-Flr-1 is buried ~10 Å from the protein surface, direct contact between FMN and the [4Fe-4S] clusters of ferredoxin is not likely to occur. We therefore postulate that electron transfer is mediated via water molecule(s). The active site cavity of Ma-Flr-1, especially at the

isoalloxazine ring system of FMN, can be accessed by waters. Water-mediated electron transfer between two redox centers has been proposed for the two copper centers of the α-amidating monooxygenase (*32*) and between cytochrome c_2 and the photosynthetic reaction center (*33*). Residue H55 forms a hydrogen bond with the N1 position of the isoalloxazine ring, properties that are suitable for participation in electron transfer via donation of a proton to N1.

Hydrogen Bond Network and Redox Properties. Ma-Flr-1 is distinct from the one-electron-carrying flavodoxins for which the semiquinone of FMN is stabilized and the redox potential of the semiquinone/hydroquinone (sq/hq) couple is lowered to less than −400 mV. These properties of FMN in flavodoxins are different from those of free FMN through interaction with the protein environment. Stabilization of the semiquinone is achieved by hydrogen bonding between the N(5)H group and the carbonyl oxygen of a peptide bond in the one-electron-reduced state (*34–36*). Destabilization of the anionic N(1) atom in the fully reduced state of flavodoxins is achieved via a hydrophobic environment and the negative charge of residues adjacent to the flavin ring which lowers the sq/hq potential (*37–39*).

Features of the FMN environment of Ma-Flr-1 favor stabilization of the hydroquinone. Solvent can freely access the isoalloxazine ring which explains the increased midpoint potential for the sq/hq couple relative to flavodoxins. Further, there is an absence of negatively charged residues adjacent to the flavin ring, and N(1) of Ma-Flr-1 has contact with the positively charged His55. The structure of Ma-Flr-1 also reveals that the backbone amide of Gly35 donates a hydrogen to N(5) of FMN in a hydrogen bond that would destabilize the semiquinone. A similar interaction has been reported for the human electron transfer flavoprotein (*40*) and the oxygen insensitive nitroreductase (*41*) that are two-electron transfer proteins. Loss of the hydrogen bond in a variant of the human electron transfer flavoprotein, which forms anionic semiquinone, increases the thermodynamic stability of semiquinone by 10-fold (*42*). In nitroreductase, the semiquinone is extremely suppressed (*43*). Protonation of N(5) that would otherwise stabilize the semiquinone appears to be disfavored by a hydrogen bond formed by donation of a hydrogen from the backbone amide of Glu165 which remains in contact with N(5) via van der Waals interaction upon reduction to the hydroquinone (*44*). The structure of Ma-Flr-1 also reveals that the proton of the N(3)H group is a donor in the hydrogen bond formed with the backbone carbonyl oxygen of Gly50. However, molecular orbital calculations of free flavin suggest that this hydrogen bond-donating site plays a limited role in flavin redox chemistry and contributes primarily to stabilization of the oxidized state (*45*).

CONCLUSIONS

A flavoredoxin from *M. acetivorans*, the first from the Archaea domain, has been characterized biochemically and the crystal structure determined. The results, combined with sequence analyses of homologues retrieved from the database, identify a family of flavoproteins with a novel flavin binding motif. The structure predicts interactions of the flavoredoxin with its redox partner ferredoxin and provides a structural basis for the observed redox properties.

ACKNOWLEDGMENT

We thank Dr. David A. Grahame for providing purified Cdh from *M. thermophila,* Hauptman-Woodward Medical Research Institute for the screening of crystallization conditions, and Dr. Hemant Yennawar for assistance with the X-ray facility.

NOTE ADDED IN PROOF

Since the submission of this manuscript, a preliminary report appeared describing the crystal structure of flavoredoxin from Desulfovibrio vulgaris. Ueda, Y., Shibata, N., Takeuchi, D., Kitamura, M., and Higuchi, Y. (2008) Crystallization and preliminary X-ray crystallographic study of flavoredoxin from Desulfovibrio vulgaris Miyazaki F. *Acta Crystallogr. Sect. F Struct. Biol. Cryst. Commun. 64*, 851−853.

SUPPORTING INFORMATION AVAILABLE

Data collection and refinement statistics for Ma-Flr-1 (Table S1), sequence alignments of representative homologues of Ma-Flr-1 (Figure S1), the phylogenetic tree of the flavoredoxin family (Figure S2), and electrostatic potential maps of Ma-Flr-1, *D. vulgaris* Flr, flavin reductase from *B. thermoglucosidasius*, and ferric reductase from *A. fulgidus.* This material is available free of charge via the Internet at http://pubs.acs.org.

REFERENCES

1. Chen, L., Ming-Yih, L., and LeGall, J. (1993) Isolation and characterization of flavoredoxin, a new flavoprotein that permits *in vitro* reconstitution of an electron transfer chain from molecular hydrogen to sulfite reduction in the bacterium *Desulfovibrio gigas*. *Arch. Biochem. Biophys. 303*, 44–50.
2. Agostinho, M., Oliveira, S., Broco, M., Ming-Yih, L., LeGall, J., and Rodrigues-Pousada, C. (2000) Molecular cloning of the gene encoding flavoredoxin, a flavoprotein from *Desulfovibrio gigas*. *Biochem. Biophys. Res. Commun. 272*, 653–656.
3. Broco, M., Marques, A., Oliveira, S., and Rodrigues-Pousada, C. (2005) Characterisation of the 11 Kb DNA region adjacent to the gene encoding *Desulfovibrio gigas* flavoredoxin. *DNA Sequence 16*, 207–216.
4. The Comprehensive Microbial Resource. J. Craig Venter Institute, http://cmr.tigr.org/tigr-scripts/CMR/CmrHomePage.cgi. (accessed January 2008).
5. Ferry, J. G., and Kastead, K. A. (2007) Methanogenesis. In *Archaea: Molecular Cell Biology* (Cavicchioli, R., Ed.) pp 288−314, ASM Press, Washington, DC.
6. Ferry, J. G. (2008) Acetate-based methane production. In *Bioenergy* (Wall, J. D., Harwood, C. S., and Demain, A., Eds.) pp 155−170, ASM Press, Washington, DC.
7. Schlesinger, W. H. (2000) The global carbon cycle. In *Biogeochemistry*, pp 308−321, Academic Press, Inc., San Diego.
8. Whitby, L. G. (1953) A new method for preparing flavin-adenine dinucleotide. *Biochem. J. 54*, 437–442.
9. Nelson, M. J. K., and Ferry, J. G. (1984) Carbon monoxide-dependent methyl coenzyme M methylreductase in acetotrophic *Methanosarcina* spp. *J. Bacteriol. 160*, 526–532.
10. Lessner, D. J., Li, L., Li, Q., Rejtar, T., Andreev, V. P., Reichlen, M., Hill, K., Moran, J. J., Karger, B. L., and Ferry, J. G. (2006) An unconventional pathway for reduction of CO_2 to methane in CO-grown *Methanosarcina acetivorans* revealed by proteomics. *Proc. Natl. Acad. Sci. U.S.A. 103*, 17921–17926.
11. Otwinowski, Z., and Minor, W. (1997) Processing of X-ray diffraction data collected in oscillation mode. In *Methods in Enzymology* (Carter, C. W., Jr., and Sweet, R. M., Eds.) pp 307−326, Academic Press, Inc., New York.
12. McCoy, A. J., Grosse-Kunstleve, R. W., Storoni, L. C., and Read, R. J. (2005) Likelihood-enhanced fast translation functions. *Acta Crystallogr. D61*, 458–464.

13. Terwilliger, T. C. (2000) Maximum-likelihood density modification. *Acta Crystallogr. D56*, 965–972.
14. Winn, M. D., Isupov, M. N., and Murshudov, G. N. (2001) Use of TLS parameters to model anisotropic displacements in macromolecular refinement. *Acta Crystallogr. D57*, 122–133.
15. Jones, T. A., Zou, J. Y., Cowan, S. W., and Kjeldgaard, M. (1991) Improved methods for building protein models in electron density maps and the location of errors in these models. *Acta Crystallogr. A47* (Part 2), 110–119.
16. Laskowski, R. A., MacArthur, M. W., Moss, D. S., and Thornton, J. M. (1993) PROCHECK: A program to check the stereochemical quality of protein structures. *J. Appl. Crystallogr. 26*, 283–291.
17. The ExPASy (Expert Protein Analysis System). Swiss Institute of Bioinformatics, http://ca.expasy.org/uniprot/Q8TTU7. (accessed January 2008).
18. Li, Q., Li, L., Rejtar, T., Lessner, D. J., Karger, B. L., and Ferry, J. G. (2006) Electron transport in the pathway of acetate conversion to methane in the marine archaeon *Methanosarcina acetivorans*. *J. Bacteriol. 188*, 702–710.
19. Li, L., Li, Q., Rohlin, L., Kim, U., Salmon, K., Rejtar, T., Gunsalus, R. P., Karger, B. L., and Ferry, J. G. (2007) Quantitative proteomic and microarray analysis of the archaeon *Methanosarcina acetivorans* grown with acetate versus methanol. *J. Proteome Res. 6*, 759–771.
20. Terlesky, K. C., and Ferry, J. G. (1988) Ferredoxin requirement for electron transport from the carbon monoxide dehydrogenase complex to a membrane-bound hydrogenase in acetate-grown *Methanosarcina thermophila*. *J. Biol. Chem. 263*, 4075–4079.
21. Fischer, R., and Thauer, R. K. (1990) Ferredoxin-dependent methane formation from acetate in cell extracts of *Methanosarcina barkeri* (strain MS). *FEBS Lett. 269*, 368–372.
22. Broco, M., Soares, C. M., Oliveira, S., Mayhew, S. G., and Rodrigues-Pousada, C. (2007) Molecular determinants for FMN-binding in *Desulfovibrio gigas* flavoredoxin. *FEBS Lett. 581*, 4397–4402.
23. Hatchikian, E. C., Bruschi, M., Forget, N., and Scandellari, M. (1982) Electron transport components from methanogenic bacteria: The ferredoxin from *Methanosarcina barkeri* (strain Fusaro). *Biochem. Biophys. Res. Commun. 109*, 1316–1323.
24. Terlesky, K. C., and Ferry, J. G. (1988) Purification and characterization of a ferredoxin from acetate-grown *Methanosarcina thermophila*. *J. Biol. Chem. 263*, 4080–4082.
25. Vadas, A., Monbouquette, H. G., Johnson, E., and Schroder, I. (1999) Identification and characterization of a novel ferric reductase from the hyperthermophilic Archaeon *Archaeoglobus fulgidus*. *J. Biol. Chem. 274*, 36715–36721.
26. Chiu, H. J., Johnson, E., Schroder, I., and Rees, D. C. (2001) Crystal structures of a novel ferric reductase from the hyperthermophilic archaeon *Archaeoglobus fulgidus* and its complex with $NADP^+$. *Structure 9*, 311–319.
27. Kirchner, U., Westphal, A. H., Muller, R., and van Berkel, W. J. (2003) Phenol hydroxylase from *Bacillus thermoglucosidasius* A7, a two-protein component monooxygenase with a dual role for FAD. *J. Biol. Chem. 278*, 47545–47553.
28. van den Heuvel, R. H., Westphal, A. H., Heck, A. J., Walsh, M. A., Rovida, S., van Berkel, W. J., and Mattevi, A. (2004) Structural studies on flavin reductase PheA2 reveal binding of NAD in an unusual folded conformation and support novel mechanism of action. *J. Biol. Chem. 279*, 12860–12867.
29. Lovenberg, W., Buchanan, B. B., and Rabinowitz, J. C. (1963) Studies on the chemical nature of clostridial ferredoxin. *J. Biol. Chem. 238*, 3899–3912.
30. De Pascalis, A. R., Jelesarov, I., Ackermann, F., Koppenol, W. H., Hirasawa, M., Knaff, D. B., and Bosshard, H. R. (1993) Binding of ferredoxin to ferredoxin:$NADP^+$ oxidoreductase: The role of carboxyl groups, electrostatic surface potential, and molecular dipole moment. *Protein Sci. 2*, 1126–1135.
31. Hurley, J. K., Hazzard, J. T., Martinez-Julvez, M., Medina, M., Gomez-Moreno, C., and Tollin, G. (1999) Electrostatic forces involved in orienting *Anabaena* ferredoxin during binding to *Anabaena* ferredoxin:$NADP^+$ reductase: Site-specific mutagenesis, transient kinetic measurements, and electrostatic surface potentials. *Protein Sci. 8*, 1614–1622.
32. Francisco, W. A., Wille, G., Smith, A. J., Merkler, D. J., and Klinman, J. P. (2004) Investigation of the pathway for inter-copper electron transfer in peptidylglycine α-amidating monooxygenase. *J. Am. Chem. Soc. 126*, 13168–13169.
33. Miyashita, O., Okamura, M. Y., and Onuchic, J. N. (2005) Interprotein electron transfer from cytochrome c2 to photosynthetic reaction center: Tunneling across an aqueous interface. *Proc. Natl. Acad. Sci. U.S.A. 102*, 3558–3563.
34. Mayhew, S. G. (1971) Studies on flavin binding in flavodoxins. *Biochim. Biophys. Acta 235*, 289–302.
35. O'Farrell, P. A., Walsh, M. A., McCarthy, A. A., Higgins, T. M., Voordouw, G., and Mayhew, S. G. (1998) Modulation of the redox potentials of FMN in *Desulfovibrio vulgaris* flavodoxin: Thermodynamic properties and crystal structures of glycine-61 mutants. *Biochemistry 37*, 8405–8416.
36. Hoover, D. M., Drennan, C. L., Metzger, A. L., Osborne, C., Weber, C. H., Pattridge, K. A., and Ludwig, M. L. (1999) Comparisons of wild-type and mutant flavodoxins from *Anacystis nidulans*. Structural determinants of the redox potentials. *J. Mol. Biol. 294*, 725–743.
37. Hall, L. H., Bowers, M. L., and Durfor, C. N. (1987) Further consideration of flavin coenzyme biochemistry afforded by geometry-optimized molecular orbital calculations. *Biochemistry 26*, 7401–7409.
38. Zheng, Y.-J., and Ornstein, R. L. (1996) A theoretical study of the structures of flavin in different oxidation and protonation states. *J. Am. Chem. Soc. 118*, 9402–9408.
39. Zhou, Z., and Swenson, R. P. (1995) Electrostatic effects of surface acidic amino acid residues on the oxidation-reduction potentials of the flavodoxin from *Desulfovibrio vulgaris* (Hildenborough). *Biochemistry 34*, 3183–3192.
40. Roberts, D. L., Frerman, F. E., and Kim, J. J. (1996) Three-dimensional structure of human electron transfer flavoprotein to 2.1 Å resolution. *Proc. Natl. Acad. Sci. U.S.A. 93*, 14355–14360.
41. Haynes, C. A., Koder, R. L., Miller, A. F., and Rodgers, D. W. (2002) Structures of nitroreductase in three states: Effects of inhibitor binding and reduction. *J. Biol. Chem. 277*, 11513–11520.
42. Salazar, D., Zhang, L., deGala, G. D., and Frerman, F. E. (1997) Expression and characterization of two pathogenic mutations in human electron transfer flavoprotein. *J. Biol. Chem. 272*, 26425–26433.
43. Koder, R. L., Haynes, C. A., Rodgers, M. E., Rodgers, D. W., and Miller, A. F. (2002) Flavin thermodynamics explain the oxygen insensitivity of enteric nitroreductases. *Biochemistry 41*, 14197–14205.
44. Nogues, I., Campos, L. A., Sancho, J., Gomez-Moreno, C., Mayhew, S. G., and Medina, M. (2004) Role of neighboring FMN side chains in the modulation of flavin reduction potentials and in the energetics of the FMN:apoprotein interaction in *Anabaena* flavodoxin. *Biochemistry 43*, 15111–15121.
45. Bradley, L. H., and Swenson, R. P. (2001) Role of hydrogen bonding interactions to N(3)H of the flavin mononucleotide cofactor in the modulation of the redox potentials of the *Clostridium beijerinckii* flavodoxin. *Biochemistry 40*, 8686–8695.

BI801012P